



## Assessment of the Impact of Annealing on the Optical Properties of Cadmium Sulfide Thin Films by Spin Coating Deposition (SCD)

Atyaf Adnan Farhan\*

Ministry of Education, Al-Karkh Second Directorate of Education, Al-Mustafa Secondary School for Distinguished Students

\*Email of the Corresponding Author: [atyafadnan8892@gmail.com](mailto:atyafadnan8892@gmail.com)

**Article history:** Received 4 Feb. 2026, Accepted 19 Mar. 2026, Published online 15 Jun. 2026

**Abstract:** Cadmium sulfide (CdS) thin films have been fabricated on glass substrates via the spin-coating method, followed by thermal annealing at 100°C, 150°C, and 200°C. Optical studies indicated that the deposited films possess high transparency in the visible and near-infrared regions, with transmittance values reaching approximately 75%. The films exhibited a direct optical band gap, which showed a gradual decrease from 2.2 eV to 1.6 eV as the annealing temperature increased. Additionally, increasing the annealing temperature resulted in noticeable improvements in film homogeneity and crystallinity. These findings underscore the crucial role of thermal annealing in modulating the optical properties of CdS thin films, thereby improving their suitability for optoelectronic applications.

**Keywords:** Spin Coating Deposition (SCD), Atomic Force Microscopy (AFM), Zinc Blende (ZB), CdS (Cadmium Sulfate).

### 1. Introduction

Cadmium sulfide (Cd S), a typical II–VI compound semiconductor, shows a unique bonding nature that combines the covalency and ionicity. In the former, a large electronegativity difference between cationic Group II (Cd) coating and the VI elements (S), endows largely ionic aspects to the almost covalent bonding. Intense electron localization, binding of lattice energies, and thereby higher thermal stability are some of the outcomes. These basic properties appear as the characteristic melting points and wide band gaps compared to covalent semiconductors of comparable atomic mass (e.g., silicon/germanium) [1].

Cadmium sulfide occurs in two major structural forms, the cubic zinc blende (sphalerite) phase and hexagonal wurtzite phase. The instability at the planar film surface is so solid that when deposited at substrate temperatures where the formation of these phases is thermodynamically stable and kinetically preferable, thin films may not form ordered phases. For CdS, the metaphase is zinc blende (ZB), which is favoured at lower substrate temperatures (300°C), the thermodynamically-stable wurtzite phase is dominant by virtue of its lower bulk free energy. This phase selectivity has important consequences for epitaxial growth, defect creation and subsequent properties [2]. Recent progress on control of phase-pure or mixed-phase films is also achieved in Fiske cells for device applications via molecular beam epitaxy (MBE) and pulsed laser deposition (PLD). The renewed and persistent interest in CdS thin films is mainly attributed to its critical function as a window material for high-efficiency thin-film photovoltaic (PV) devices, including predominantly heterojunctions with semiconductor absorbers like CdTe and



Cu(In,Ga)Se<sub>2</sub> (CIGS) [3,4]. Its appropriateness is based on a combination of key features: the direct band gap (~2.42 eV at room temperature), that lies comfortably in the solar spectrum well below its absorption edge; high (it exceeds 10<sup>4</sup> cm<sup>-1</sup>) absorption coefficient for photon energies larger than the band gap, which should enable efficient carrier generation in ultrathin layers; and favorable interface energetics with leading absorber materials to promote successful carrier separation. These properties have allowed certified solar cell conversion efficiencies in CdTe devices in excess of 22% and for CIGS they are around 23%, with the key component of recently recorded efficiency architectures remaining a CdS layer [5,6]. Apart from photovoltaic applications, due to the tunable band gap (by alloying with Zn or Se) and the strong excitonic effects, CdS is of interest for light-emitting diodes (LEDs), photodetectors and nonlinear optical devices.

Cadmium sulfide is a congruently sublimating material at around 700 °C or higher and melts at high pressure near 1750°C, allowing for fabrication with a wide range of techniques including thermal evaporation, chemical bath deposition (CBD), sputtering and close-spaced sublimation (CSS). The static dielectric constant of the material is ~11.6, and its density is 4.84 g/cm<sup>3</sup>. A defining and technologically important characteristic of CdS is its inherent n-type conductivity in as-deposited films. This conductivity is due to intrinsic defects, primarily sulfur vacancies (V<sub>S</sub>) and cadmium interstitials (Cd<sub>i</sub>), acting as shallow donors. On the other hand, successful p-type doping is challenging—a typical example of the problem of “doping asymmetry” in large band-gap II-VI compounds. This is due to the presence of strong self-compensation mechanisms, which leads to a decrease in the formation energy of native acceptor (e.g., Cd vacancy, V<sub>Cd</sub>) upon n-type doping or compensating donor defects spontaneously appearing against desired p-type dopants such as Na or N [7,8]. This asymmetry inherently results in the hindrance of CdS homojunction device.

The microstructure of the polycrystalline CdS films is closely related to their electrical and optical properties. Undoped single-crystal CdS has resistivity values as high as 10<sup>12</sup> Ω·cm, whereas polycrystalline films usually show lower resistivity because of grain boundary conduction and native defects. Doping control with group III (In, Al, Ga) [10] or halogen (Cl, Br) can decrease the resistivity to the order of 10<sup>-3</sup>–10<sup>-1</sup> Ω·cm, which is essential for low-resistance window layers [9]. Grain size, which is usually in the 0.3–0.5 μm range for standard thicknesses, plays a crucial role in determining the carrier mobility, recombination and optical scattering of a material. In particular, post-deposition thermal annealing is crucial for promoting grain growth, suppressing the density of grain boundaries and passivating intra-grain defects. A significant step in CdTe PV processing is CdCl<sub>2</sub> vapor or solution treatment before annealing. This chloride treatment significantly increases recrystallization, facilitates grain boundary passivation (most likely via the generation of CIS donors that compensate deep traps), and optimizes the electronic structure at the CdS/CdTe interface, resulting in large enhancements in VOC and FF [10,11]. Recent investigations include interface engineering with ultrathin (<50 nm) CdS layers or CdS:O alloys to reduce parasitic absorption and improve the blue-response of the solar cells

## 2. Materials and methods

In the present work, CdS thin films have been deposited onto glass substrates using the spin-coating technique. This method involves dispensing a precursor solution onto the glass substrate, followed by high-speed rotation to achieve uniform film deposition. After deposition, the films have been subjected to thermal annealing at different temperatures in order to investigate the effect of annealing temperature on their structural and optical properties.

### 2.1. Devices and Materials.

Cadmium sulfide (CdS) was obtained from Sigma-Aldrich (Germany), and a sensitive scale with four digits, an electric oven with high temperature control, a magnetic stirrer, and a spin coating device.

### 2.2. Film Deposition by Spin Coating Technique

The three main physical stages of spin-coating are (i) deposition and spin-up, (ii) spin-off or viscous flow, and (iii) solvent evaporation. The method commences deposition of a precursor solution onto a



substrate or Slowdive from a syringe or nozzle. The substrate is then quickly sped up to the desired rotation speed. In this early phase, centrifugal forces are the dominant factor driving the solution away radially. This leads to a rapid, exponential decay in film thickness with the extra removed liquid being expelled from the edges of the substrate until an equilibrium metastable fluid layer is formed.

After uniform spreading, the film-thinning rate enters into a regime determined by the competition between centrifugal drainage and viscous resistance. Although solvent evaporation also takes place, the dominating mechanism for thickness decrease is still the viscous flow of solution across the substrate due to centrifugal force. The thickness decays as  $t^{-1/2}$ , where  $t$  is time. In the last stage, viscous flow is suppressible because the solution viscosity dramatically increases owing to solvent evaporation. Additional thinning and drying are primarily governed by the solvent evaporation rate, which results in film contraction to form a dry solid film. It should be noted that these stages are not isolated and considerable overlap in time is present, especially between the spin-off and evaporation stages since solvent evaporation occurs throughout the entire process [12]. The resulting DFT ( $h$ ) follows a known inverse-power relationship with the square root of the spin speed ( $\omega$ ), typically of the form  $h \propto \omega^{-1/2}$  and diminishes logarithmically in time as spinning progresses through its mid-stage (=the dominant spin-off phase). This relationship is depicted schematically in Fig. 1.

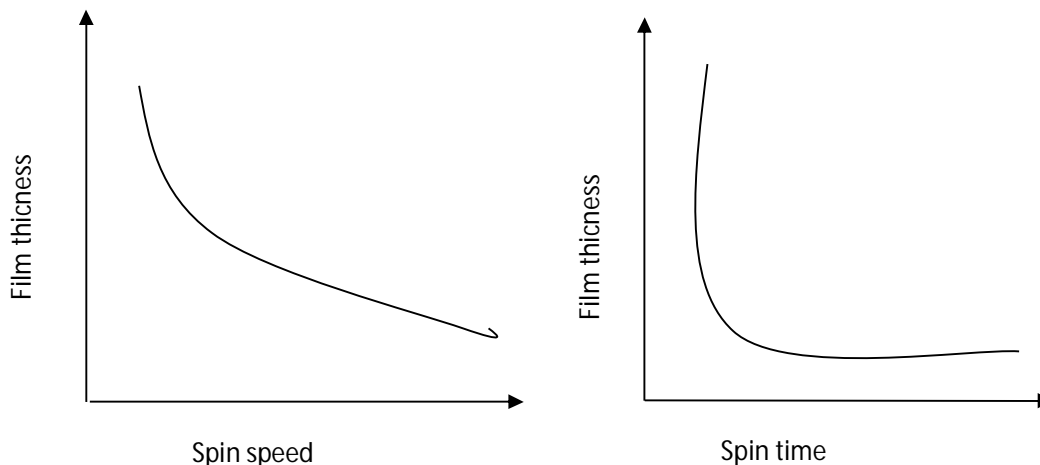


**Fig.1:** The relation between film thickness and both spin speed and spin time.

### 2.3. Preparing the Chemicals

Analytical-grade chemicals supplied by BDH were used in the present study. The specifications and chemical parameters of the materials employed are listed in table 1.

**Table 1.** List of used materials.

Material	atomic weight	Purity	Chemical Composition	Concentration	Company
Cadmium Nitrite	308.47	99%	$Cd(NO_3)_2 \cdot 4H_2O$	0.60 M	BDH
Thiourea	76.12	99%	$Cs(NH_2)_2$	1.0 M	BDH
Polyvinyl alcohol (PVA)	1400	99%			BDH

## 2.4. Synthesis of CdS/PVA Nanocomposite Thin Films

Thin films of cadmium sulfide polyvinyl alcohol (PVA) matrix nanocomposite have been produced on glass substrate by using the spin coating method. The cadmium source was cadmium acetate tetrahydrate  $[\text{Cd}(\text{NO}_3)_2 \cdot 4\text{H}_2\text{O}]$  and the sulfur precursor used was thiourea  $[\text{CS}(\text{NH}_2)_2]$ . Stoichiometric 3:5 (Cd:S) molar ratio was used, with polyvinyl alcohol PVA serving as a host polymer matrix and stabilizer of particle growth and aggregation.

The cation/anion ratio of the Cd:S precursor is one of the most crucial synthetic factors, which is directly responsible for a particular crystallographic phase of the CdS formed. The presence of high sulphur concentration has been demonstrated to promote hexagonal (wurtzite) phase formation, which is usually beneficial for photovoltaic applications because of its electronic properties; while the presence of high cadmium concentration favours cubic (zinc blende) phase stability [13]. The synthesis procedure includes preparation of a precursor matrix by mixing 20 mL of aqueous cadmium acetate solution (0.6 M) with an equal volume of aqueous PVA solution (5% w/v).

The resulting colourless solution was continuously magnetically stirred at 70 °C for 90 min and further aged overnight to afford a homogeneous transparent product, indicating complete incorporation of the cadmium precursor into the polymer matrix. Then, 20 mL of a 1 M thiourea solution was added dropwise with vigorous stirring for another 30 min to start the reaction. Before deposition, the glass substrates were cleaned with a common chemical cleaning process. Then the precursor solution prepared naturally was spin-coated on the substrates. Wet films were then thermally annealed (after deposition) in an ordinary oven at 100 °C, 150 °C and 200 °C. Colouration of the transparent films tints light yellow between 15–20 min during thermal annealing, indicative of NPs being in situ generated within PVA matrix. In this hybrid material, the PVA not only forms a stable and uniform film but also passivates the nanoparticle surfaces, preventing Ostwald ripening and leading to a homogeneous dispersion.

## 3. Results and discussion

### 3.1. X-Ray Diffraction (XRD) Analysis

The structural properties of the spin-coated CdS thin films have been examined using X-ray diffraction (XRD) with  $\text{CuK}\alpha$  radiation. Figures 2, 3, and 4 present the XRD patterns of CdS thin films annealed at 100 °C, 150 °C, and 200 °C for 10–15 minutes, respectively.

The XRD patterns of the annealed samples exhibit diffraction peaks at approximately 24.16°, 20.94°, and 22.00°, corresponding to the characteristic reflections of CdS. The presence of relatively weak and broadened diffraction peaks indicates the formation of nanocrystalline CdS films. The broadening of the diffraction peaks is attributed to the small crystallite size, as peak width increases with decreasing particle size due to size-related effects.

Terminal annealing effect on structural features of the CdS/PVA nanocomposite films is shown in Table 1. The crystalline size, as calculated from X-ray diffraction (XRD), demonstrates a positive link with the annealing temperatures as list in table 2. In particular, as the annealing temperature temperatures from 100 °C to 200 °C, the average crystallite size increases from around ~29.97 nm to ~32.90 nm which can be attributed to the improvement of atomic mobility and grain coalescence of smaller grains at high temperature due to minimization for the total surface free energy balance. The comparative summary of crystallite size (via XRD) and optical band gap ( $E_g$ ) values of the films annealed at different temperatures are summarized in Table 2.

The correlation between these two parameters provide important information about the quantum confinement effect. In general, a decrease of the optical band gap with increasing crystallite size has been observed for semiconductor nanocrystals when their particle size reaches or exceeds the value of the Bohr exciton radius which is believed to indicate loss of quantum confinement.



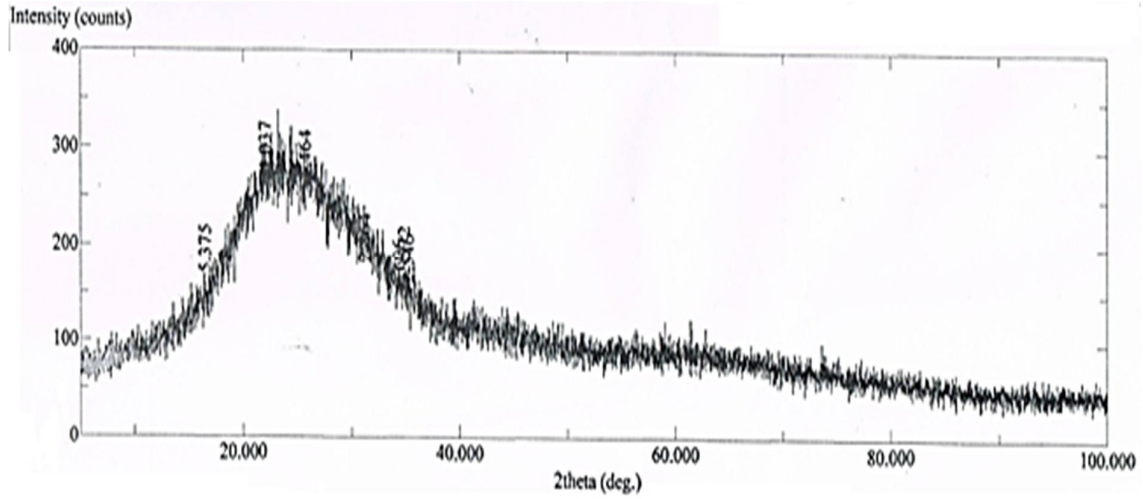


Fig.2: Shows the X-ray diffraction for CdS at 100C°

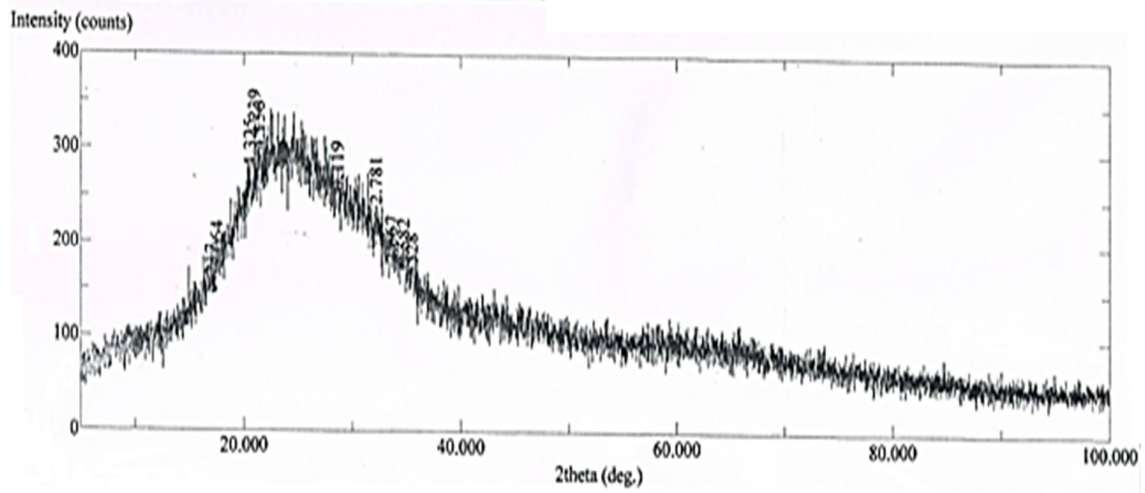


Fig.3: Shows the X-ray diffraction for CdS at 150C°

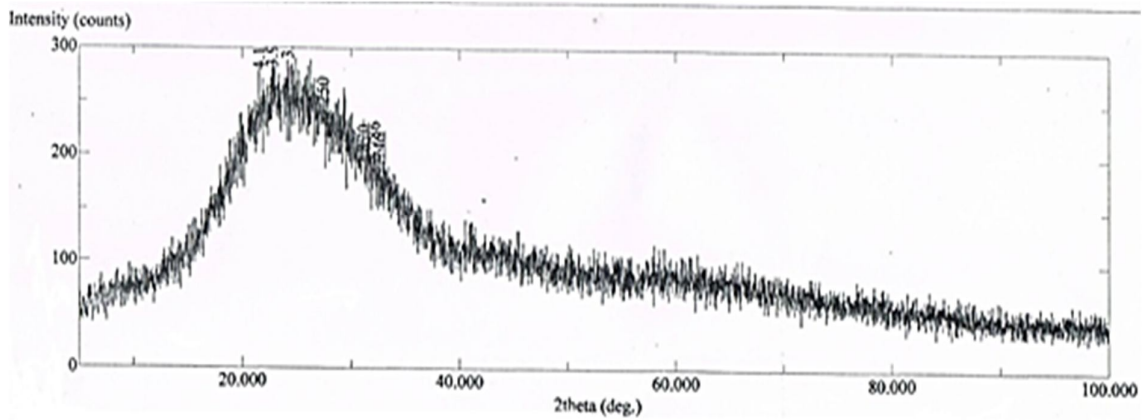


Fig.4: Shows the X-ray diffraction for CdS at 200C°

**Table 2.** XRD pattern for CdS thin films with different values of annealing temperature.

Annealing Temp (°C)	2 $\theta$ (Deg.)	FWHM (Deg.)	d <sub>hkl</sub> (Å)	Intensity	I/I <sub>o</sub>	hkl	Card no.
100	16.480	0.259	3.1743	169	62	113	00-041-1049
	22.000	0.282	4.0369	274	100	230	00-010-0454
	25.700	0.282	3.4635	266	98	311	00-041-1049
150	20.520	0.329	4.3246	279	90	113	00-041-1049
	20.940	0.259	4.2388	310	100	230	00-010-0454
	21.360	0.282	4.1564	297	96	311	00-010-0454
200	22.740	0.353	3.9072	281	98	200	00-010-0454
	24.160	0.259	3.6807	289	100	230	00-010-0454
	27.420	0.259	3.2500	234	81	112	00-041-1049

These results prove that the thermal annealing treatment is a reliable process to adjust the microstructural and, hence, the optoelectronic characteristics of the CdS/PVA nanocomposite films prepared are shown in Table 2.

**Table 3.** Values of grain size and energy gap V.S. annealing temperatures.

Ta ( C)	Grain No	Avg. Diameter (nm)
100	52	224.45
150	45	212.86
200	81	156.23

**Table 4.** Average diameter for samples grains at different Ta

Annealing temperature (°c)	Grain size from XRD (nm)	Energy gap (eV)
100	29.97	2.25
150	32.58	1.65
200	32.897	1.60

### 3.2. Atomic Force Microscopy (AFM)

Fig 5 (a, b & c) shows the atomic force microscopic picture for the three samples at different annealing temperatures Ta=100, 150, and 200 C, respectively. The grain size and the average diameter were listed in Table 4.



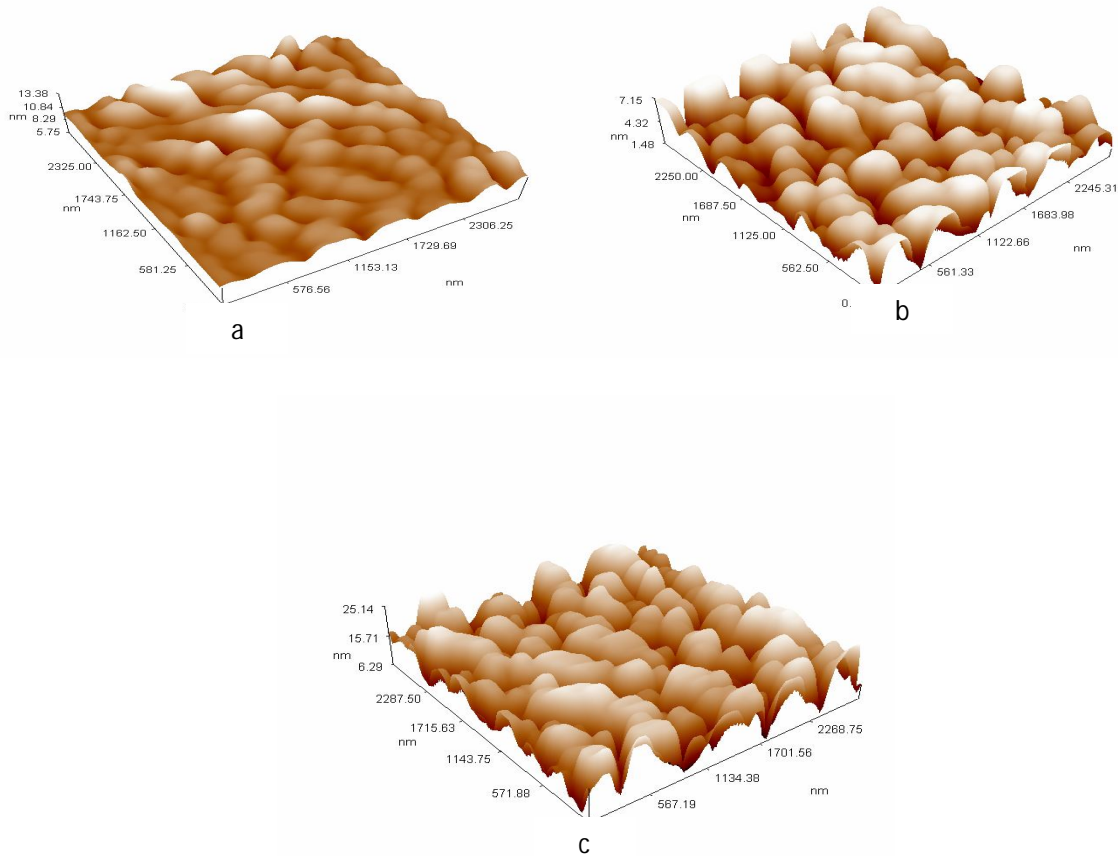


**Fig.5:** AFM for a) 1<sup>st</sup> simple at T=100 C<sup>0</sup>, b) 2<sup>nd</sup> simple at T=150 C<sup>0</sup>, c) 3<sup>rd</sup> simple at T=200 C<sup>0</sup>.

### 3.3 Optical Measurements

#### 3.3.1 Transmittance Spectra

The optical transmittance of the CdS films has been measured at avroom temperature in the 300–1100 nm wavelength range shown in Figure 6. Most of the prepared films possess high optical transparency in the visible and near infrared ranges, with transmittance over 85% for all.

A gradual reduction in the optical transmittance is seen with increasing annealing temperature, and this data is summarized table 4. This decrease is related to the micro structuring evolution of the films. The improvement of sub crystallinity, grain size and texture (XRD) are all confirmed for the post-deposition annealing. These microstructural enhancements contribute to an increased volume fraction of crystalline material and a decrease in the amount of light scattering at grain boundaries that can be directed toward in-plane optical modes, resulting in a higher effective optical path length and inner absorption within the films. As a result, the annealed films show higher photon absorbing ability reflected with the measured decrease in total transmittance.



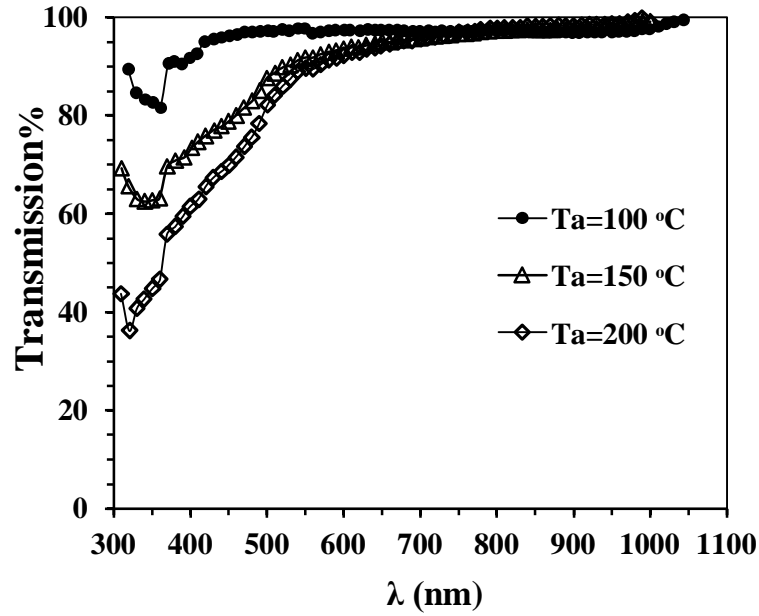


Fig.6: Transmittance spectra of CdS thin films annealed at different temperatures.

### 3.3.2. Optical Energy Gap

The optical energy gap ( $E_g$ ) of the CdS thin films has been calculated using the Tauc formula. In order to investigate the nature of the optical transition,  $(\alpha h\nu)^2$  was plotted as a function of photon energy ( $h\nu$ ), where  $\alpha$  represents the absorption coefficient. Extrapolation of the high-absorbing region in the plot to the energy axis resulted in a straight line, verifying a direct allowed transition for CdS. The calculated optical band gap is shown in Fig.7.

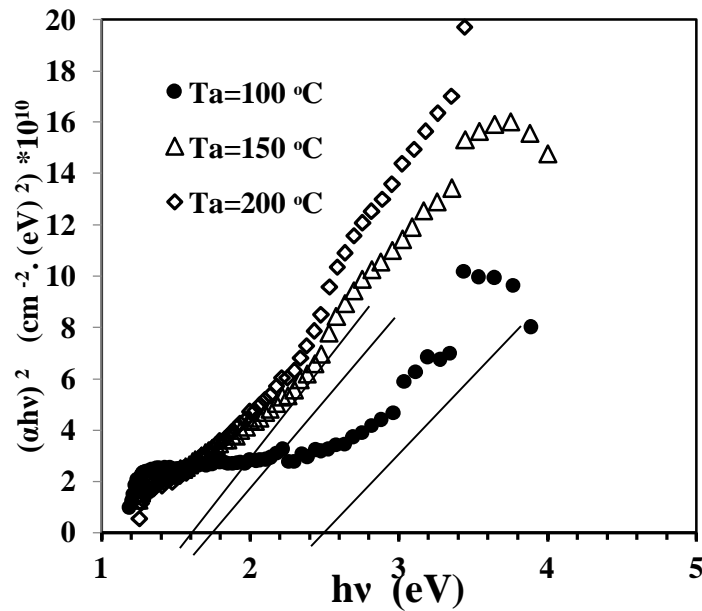


Fig.7: Tauc plots for determining the optical energy gap of CdS thin films annealed at different temperatures.

The optical band gaps of all the samples are respectively 2.3 eV for the unannealed one, and decrease with elevated annealing temperature ( $T_a$ ). This discovered band gap reduction may be associated with the microstructural evolution of the films following annealing. In contrast, high grain growth and good crystallinity are achieved with the increase of annealing temperature, as verified from XRD. The resulting increase in the crystallite size is responsible for a suppression of quantum confinement effects, which are extremely strong in nanostructured semiconductors. Besides, as the lessened structural disorder and defect density (due to better crystallinity) reduces the density of localized tail states close to the band edge, such a change leads to a clear optical band gap increase.

### 3.3.3. Optical and Structural Parameters

All calculated optical and structural parameters of the CdS thin films annealed at different temperatures are summarized in Table 5.

**Table 5.** Calculations of the Optical and structural properties at different temperatures

Parameters	T=100 C <sup>0</sup>	T=150 C <sup>0</sup>	T=200 C <sup>0</sup>
Grain size	29.9	32.58	32.9
Absorption of films	0.011	0.028	0.035
Transmission spectra	97.427%	93.691%	92.235%
Optical Energy Gap	2.25	1.65	1.60

## 4. Conclusion

CdS/PVA nanocomposite thin films were successfully fabricated using the spin-coating technique, and the effect of thermal annealing on their structural and optical properties was investigated. XRD analysis showed an increase in crystallite size with increasing annealing temperature, indicating improved film crystallinity. Optical studies revealed enhanced absorption and a corresponding decrease in transmittance as the annealing temperature increased. Additionally, the optical energy gap exhibited a noticeable reduction with increasing annealing temperature. These findings demonstrate that thermal annealing is an effective approach for tuning the properties of CdS/PVA thin films for optoelectronic applications.

## Ethics Approval and Consent for Authors

I acknowledge that I have completed my research in accordance with the ethics of scientific research and submitted my research paper, which aims to serve the community.

## Author declaration

I, Atyaf Adnan Farhan, hereby declare that I am the sole owner of the intellectual property rights to the research manuscript titled "[Assessment of the Impact of Annealing on the Optical Properties of Cadmium Sulfide Thin Films by Spin Coating Deposition (SCD)]" submitted for publication in the Iraqi Journal of Laser.

## References

- [1] Vanalakar, S.A., Patil, V.L., Patil, S.M., Deshmukh, S.P., Patil, P.S., and Kim, J.H., Chemical and gas sensing property tuning of cadmium sulfide thin films. *Materials Science and Engineering: B*, **282**, p.115787 (2022), <https://doi.org/10.1016/j.mseb.2022.115787>.
- [2] A. I. Khudiar, S. M. Zulfequar and Z. H. Khan, *Chalcogenide Letters*, **7**, 291-298 (2010). [https://chalcogen.ro/291\\_Kudhiar.pdf](https://chalcogen.ro/291_Kudhiar.pdf)
- [3] D. Saikia, P. K. Gogoi and P. K. Saikia: *Chalcogenide Letters*. **7**, 317-323 (2010). <https://pubs.acs.org/doi/abs/10.1021/cm990362%2B>
- [4] V. B. Sanap and B. H. Pawar: *Chalcogenide Letters*. **6**, 415-419 (2009). [https://chalcogen.ro/419\\_Sanap-sept.pdf](https://chalcogen.ro/419_Sanap-sept.pdf)

- [5] M. Thambidurai, N. Murugan, N. Muthukumarasamy, S. Agilan, S. Vasantha and R. Balasundaraprabhu: J. Mater. Sci. Technol. **26**, 193-199 (2010).
- [6] D. Nesheva, Z. Aneva, S. Reynolds, C. Main and A. G. Fitzgerald: Journal of Optoelectronics and Advanced Materials. **8**, 2120-2125 (2007). <https://www.researchgate.net/publication/303876337>.
- [7] Faris, Mina Mohammed, and Asmaa Kadim Ayal. "Electrochemical Synthesis of Fe-doped TiO<sub>2</sub> Nanotube for Gas Sensor Application." Iraqi Journal of Science **66**, 5, 1437-1450 (2025). DOI: 10.24996/ij.s.2025.66.4.4
- [8] Yildirim, E., Ozmen, S.I., Havare, A.K. and Gubur, H.M., Substrate effect on nanowall-structured CdS thin films obtained by CBD: Structural, optical, and electrochemical characterization for next-generation optoelectronic applications. Materials Chemistry and Physics, **348**, 1311-51. (2026) <https://doi.org/10.1016/j.matchemphys.2025.131651>.
- [9] Hur, S.G., Kim, E.T., Lee, J.H., Kim, G.H. and Yoon, S.G., Characterization of photoconductive CdS thin films prepared on glass substrates for photoconductive-sensor applications. Journal of Vacuum Science & Technology B: Microelectronics and Nanometer Structures Processing, Measurement, and Phenomena, **26**(4), 1334-1337(2008) <https://doi.org/10.1116/1.2945301>.
- [10] Bhusan, S., & Oudhia, A.. Photoconductivity and photoluminescence studies of chemically deposited CdS-Se: CdCl<sub>2</sub>, Ho/Nd films. Indian Journal of Pure & Applied Physics, **47**(1), 60. (2009) [https://d1wqtxts1zle7.cloudfront.net/75805510/IJPAP\\_20471\\_2060-65-libre.pdf](https://d1wqtxts1zle7.cloudfront.net/75805510/IJPAP_20471_2060-65-libre.pdf)
- [11] Oliva, A.I., Castro-Rodriguez, R., Solis-Canto, O., Sosa, V., Quintana, P. and Pena, J.L., Comparison of properties of CdS thin films grown by two techniques. Applied surface science, **205**(1-4), 56-64. (2003) [https://doi.org/10.1016/S0169-4332\(02\)01081-4](https://doi.org/10.1016/S0169-4332(02)01081-4)
- [12] Faris, M.M. and Ayal, A.K. Effect of voltage on gas sensor performance of anodization synthesized TiO<sub>2</sub> nanotubes arrays. Iraqi Journal of Science, **64**, 6135-6147(2023). DOI: 10.24996/ij.s.2023.64.12.5
- [13] M.Zambuto: Semiconductor Device (McGraw-Hill Book Company, USA, (1989).
- [14] Haider, A.J., Mousa, A.M. and Al-Jawad, S.M. Annealing effect on structural, electrical and optical properties of CdS films prepared by CBD method. Journal of semiconductor technology and science, **8**(4), 326-332, (2008) [https://d1wqtxts1zle7.cloudfront.net/50225322/Year2008Volume08\\_04\\_08-libre.pdf?1478764913](https://d1wqtxts1zle7.cloudfront.net/50225322/Year2008Volume08_04_08-libre.pdf?1478764913)
- [15] Kennedy, A., Kumar, V.S. and Raj, K.P., Chemical spray deposition technique of antimony (Sb) doped polycrystalline MnIn<sub>2</sub>S<sub>4</sub> thin films: Preparation and characterization. Materials Letters, **195**, pp.96-99. (2017) <https://doi.org/10.1016/j.matlet.2017.02.107>
- [16] Al-Douri, A.A.,. Annealing temperature effect on the structural and optical properties of thermally deposited nanocrystalline CdS thin films. Iraqi Journal of Physics, **10**(18), 111-116(2012). <https://www.ijp.uobaghdad.edu.iq/index.php/physics/article/view/756/542>
- [17] Akintunde, J.A., Effects of deposition parameters and conditions on the physical and electro-optical properties of buffer solution grown CdS thin films. physica status solidi (a), **179**(2), 363-371(2000) [https://doi.org/10.1002/1521-396X\(200006\)179:2<363::AID-PSSA363>3.0.CO;2-L](https://doi.org/10.1002/1521-396X(200006)179:2<363::AID-PSSA363>3.0.CO;2-L)
- [18] D. A. Newmen: Semiconductor Physics and Devices. Richard D. IRWIN, INC., USA (1992).
- [19] Heo, J., Ahn, H., Lee, R., Han, Y. and Kim, D., Influence of ITO surface modification on the growth of CdS and on the performance of CdS/CdTe solar cells. Solar Energy Materials and Solar Cells, **75**(1-2), 193-201(2003) [https://doi.org/10.1016/S0927-0248\(02\)00155-1](https://doi.org/10.1016/S0927-0248(02)00155-1).
- [20] N. Mott and E. Davis: Electronic Process in Non-Crystalline Materials (Oxford University Press, 2nded. (1980).
- [21] T.S.Moss: Semiconductor Opto-electronics (Butter Worths Sci. publishing, London (1973).
- [22] Muhammed Abdurraheem, Sunday Ajani, Wasiu Yahya, Godwin Egbeyale, Computational Approach to the Study of Photon Attenuation Shielding Parameters of Perovskite Ceramics , Iraqi Journal of Physics: **23**, 4 (2025) <https://www.ijp.uobaghdad.edu.iq/index.php/physics/article/view/1518>
- [23] Ali, M.M., Abbas, S.J. and Al-Kabbi, A.S., Effect of Annealing Temperature on Structural and Optical Properties of CdS Thin Films Prepared by CBD and Thermal Evaporation Techniques. Journal of Basrah Researches (Sciences), **45**(1), (2019) <https://iasj.rdd.edu.iq/journals/uploads/2024/12/08/0de7bd73c8b0ee38f2e20224b6867f60.pdf>

## تقييم تأثير التلدين على الخصائص البصرية للأغشية الرقيقة من كبريتيد الكاديوم بواسطة الترسيب بالطلاء الدوراني (SCD)

أطياف عدنان فرحان \*

وزارة التربية والتعليم / مديرية الكرخ الثانوية للتربية والتعليم / مدرسة المصطفى الثانوية للطلاب المتفوقين

البريد الإلكتروني للباحث: [atyafadnan8892@gmail.com](mailto:atyafadnan8892@gmail.com)



**الخلاصة:** تم تصنيع أغشية رقيقة من كبريتيد الكاديوم (CdS) على ركائز زجاجية باستخدام طريقة الطلاء الدوراني، ثم خضعت لمعالجة حرارية عند درجات حرارة 100 و150 و200 درجة مئوية. أشارت الدراسة البصرية إلى أن الأغشية المترسبة تتمتع بشفافية عالية في نطاق الضوء المرئي والأشعة تحت الحمراء القريبة، حيث بلغت قيم النفاذية حوالي 75%. أظهرت الأغشية فجوة نطاق ضوئي مباشرة، والتي انخفضت تدريجياً من 2.2 إلكترون فولت إلى 1.6 إلكترون فولت مع ارتفاع درجة حرارة المعالجة. بالإضافة إلى ذلك، أدى رفع درجة حرارة المعالجة إلى تحسينات ملحوظة في تجانس الأغشية وبلوريتها. تؤكد هذه النتائج على الدور المحوري للمعالجة الحرارية في تعديل الخصائص البصرية لأغشية CdS الرقيقة، مما يحسن من ملاءمتها للتطبيقات الكهروضوئية.